

THE PENNSYLVANIA STATE UNIVERSITY
SCHREYER HONORS COLLEGE

DEPARTMENT OF MECHANICAL ENGINEERING

IMPACT OF CENTERBODIES ON THE PRECESSING VORTEX CORE
IN SWIRLING FLOW

JACKSON THOMAS HORIGAN
SPRING 2021

A thesis
submitted in partial fulfillment
of the requirements
for a baccalaureate degree
in Mechanical Engineering
with honors in Mechanical Engineering

Reviewed and approved* by the following:

Jacqueline O'Connor
Associate Professor of Mechanical Engineering
Thesis Supervisor

Jean-Michel Mongeau
Assistant Professor of Mechanical Engineering
Honors Adviser

* Electronic Approvals on file.

ABSTRACT

Gas turbine combustion systems are susceptible to combustion instability, or the coupling between combustor acoustics and flame heat release rate oscillations, which can damage the combustor if oscillation amplitudes are not controlled. The dynamic structure in typical combustor flow fields is the precessing vortex core (PVC), which can interact with the thermoacoustic combustion instability oscillations. Some studies have shown that it can enhance these destructive instabilities, while others from our lab at Penn State have provided evidence that it can suppress combustion instability. Combustor designers can use different geometries and fuel injection hardware to minimize the negative contributions the PVC has on the flow. One such piece of hardware is a centerbody, a cylindrical mass that is placed ahead of the swirler in the combustor to disturb the vortex breakdown bubble and further stabilize the flame by creating a low-velocity region immediately ahead of it. Determining the impact of centerbodies on combustor flow fields, particularly the precessing vortex core, would be useful for designers, as they would gain more understanding of how the dynamic properties of the flow will change and can more accurately predict combustor performance. Prior research hypothesizes that the presence of a centerbody should suppress the PVC by disrupting the wavemaker region of the flow immediately ahead of the central recirculation zone. This work investigates the impact of different geometry centerbodies on non-reacting, variable-swirl air flow. Acoustic signals from the flow are analyzed to characterize PVC frequencies at different swirl numbers. The goal of this work is to better understand how centerbodies of different designs affect the PVC.

TABLE OF CONTENTS

LIST OF FIGURES	iii
LIST OF TABLES	iv
ACKNOWLEDGEMENTS	v
Chapter 1 Motivation	1
Chapter 2 Literature Review	5
Swirling Flow	7
Precessing Vortex Cores in Swirling Flows	10
Combustion Instability	11
Centerbodies	14
Gaps in the Literature	16
Chapter 3 Experimental Methods	17
Experimental Facility	17
New Centerbody Design	19
Diagnostics and Data Analysis	21
Chapter 4 Acoustic Characterization of the Non-Centerbody Case	22
Chapter 5 Acoustic Characterization with Centerbodies	28
Chapter 6 Conclusions and Future Work	32
BIBLIOGRAPHY	35

LIST OF FIGURES

Figure 1: Sources of US electricity generation by fuel type [1]	2
Figure 2: US electricity generation by energy source from 1950 to 2020, Colors: Dark brown – Coal, Blue – Natural Gas, Red – Nuclear, Green – Renewables, Tan – Petroleum [1] ...	3
Figure 3: Swirling flow combustor in a Siemens gas turbine [10]	5
Figure 4: Axial-Flow Swirler [11]	7
Figure 5: Radial-Flow Swirler [11].....	7
Figure 6: Non-reacting swirling flow with key structures outlined [12].....	8
Figure 7: Bubble-form vortex breakdown [16].....	9
Figure 8: Spiral-form vortex breakdown [16].....	9
Figure 9: 3D Illustration of PVC [15].....	10
Figure 10: Combustion instability feedback loop	12
Figure 11: Driving mechanism resulting in pressure waves [22]	12
Figure 12: Example of a coupling mechanism [22].....	13
Figure 13: Recirculation zone patterns due to an axially placed centerbody, as case number increases, swirl number increases and changes the flow response [24].....	15
Figure 14: Swirling flow testing rig with x , r , and θ as the axial, radial, and azimuthal axes, respectively [26].....	17
Figure 15: Swirler [28].....	18
Figure 16: Cutaway of the swirl rig with the baseline centerbody.....	19
Figure 17: Tapered Centerbody (Recessed 0.4")	21
Figure 18: Non-tapered Centerbody (Recessed 0.4")	21
Figure 19: Acoustic characterization of rig done by Frederick [28].....	23
Figure 20: Acoustic response of the PVC at 65-degree BA and various flow velocities [28].	24
Figure 21: PSD Frequency Response.....	25
Figure 22: Non-centerbody acoustic response vs. Strouhal number at $S = 1.43$	27
Figure 23: Recessed centerbody comparison at $S = 0.95$	29

Figure 24: Recessed centerbody comparison at $S = 1.15$	30
Figure 25: Protruded centerbody compared to base case at $S = 0.95$	31
Figure 26: Particle image velocimetry in the r - x plane [28]	33

LIST OF TABLES

Table 1: Centerbody Design Criteria	20
Table 2: Frederick Test Matrix [28].....	25
Table 3: Test matrix for acoustic characterization with centerbodies.....	29

ACKNOWLEDGEMENTS

I would like to thank Dr. O'Connor for being an incredible advisor and mentor throughout these years. When I joined the Reacting Flow Dynamics Laboratory in August 2019 as a junior mechanical engineering student, I was quickly thrust into the world of precessing vortex cores, boundary layers, and combustion theory. I learned what it takes to excel in this challenging field and will be forever grateful for Dr. O'Connor's dutiful and insightful guidance. These words cannot truly sum up my gratitude for all you have done for me as a student and person. You have influenced my life in many ways and taught me important lessons I will treasure for the rest of my professional career.

I would also like to thank my colleagues at the Reacting Flow Dynamics Laboratory, Ashwini Karmarkar and Joseph Molnar. They were always willing to show me how the swirl rig would perform, how to take data, or troubleshoot when the experiment needed adjustment, often at odd times of the day. I wish you both continued success in your academic and professional careers.

Finally, I would like to thank my family for all that they have done throughout my life. From my parents and brothers to my grandparents and all the Walsh and Horigan cousins, you all showed me what it means to be a man of integrity, determination, and most importantly optimism and humor. Through my family, I learned what it means to strive for audacious goals and tackle daunting challenges with poise and confidence. While these past few years have been the most challenging ones we have faced as a family, we came out closer in spirit than ever, even when quarantines and social distancing may have kept us apart in person. This thesis is my way of showing that we can still accomplish wonderful things even when faced with seemingly insurmountable odds.

Chapter 1

Motivation

In light of growing concerns of climate change, power generation from coal has been steadily replaced with that of natural gas. In the United States in 2019, gas turbines produced ~38% of electricity, and their contribution is growing over the coming decades [1]. Figure 1 shows US electricity generation broken down by fuel type. The American power grid has three components: base-load generation, adjustable-load generation, and spontaneous renewable generation. Coal and nuclear generators produce base-load power because those sources take a long time to change their power output. They cannot swing up and down with the changes of demand, and hence produce their max power (or base power) and rarely stray from it. Renewable energy generators like wind and solar farms are not as predictable as fossil fuels, and will either be on or off. Renewable generation's instability provides a niche for adjustable-load generation. This adjustable load can be, and often is, fulfilled by natural gas turbines. The turbines can change their output relatively quickly compared to base load generators and are used to fill the gaps in demand when renewable sources are not running.

Figure 2 shows the historical energy mix for the United States [1]. Note the natural gas portion in blue and how it has grown considerably since 2008. Traditional power plants typically have a service life of 50-70 years. Coal power plants commissioned in the 1970s and earlier are nearing the end of their operational lifespan and have grown costly and inefficient. This inefficiency comes from two sources: price of fuel, and cost to operate. The price of natural gas has steadily declined since 2005 and is now competitive with coal [2]. Also, operating costs of a

coal plant are significantly higher than that of a natural gas power plant of similar power output [3], [4]. The inefficiency of coal generators compared to natural gas generators has caused natural gas to be how the majority of American electricity is generated.

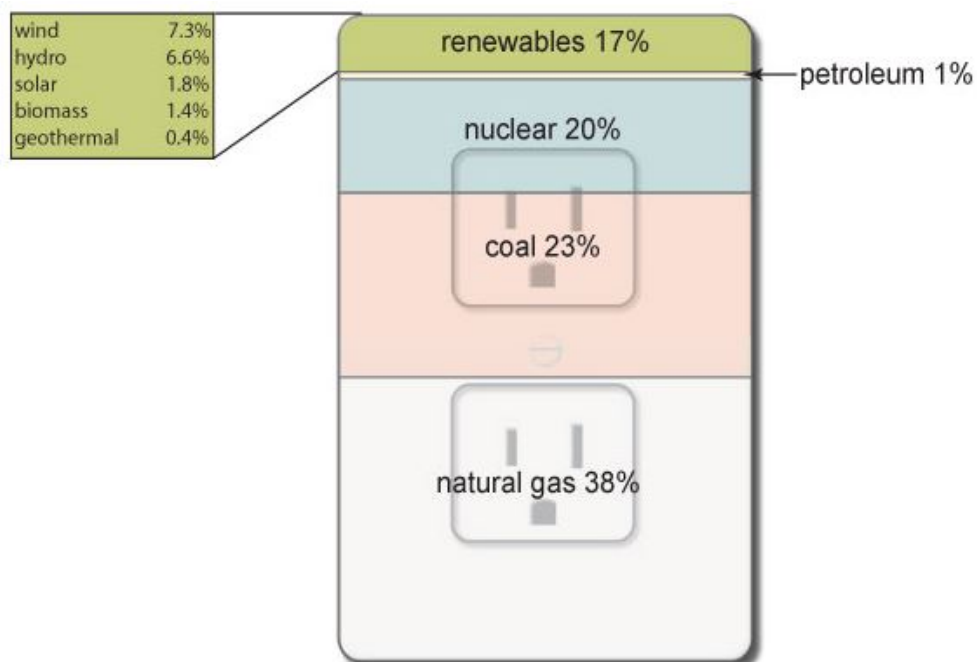


Figure 1: Sources of US electricity generation by fuel type [1]

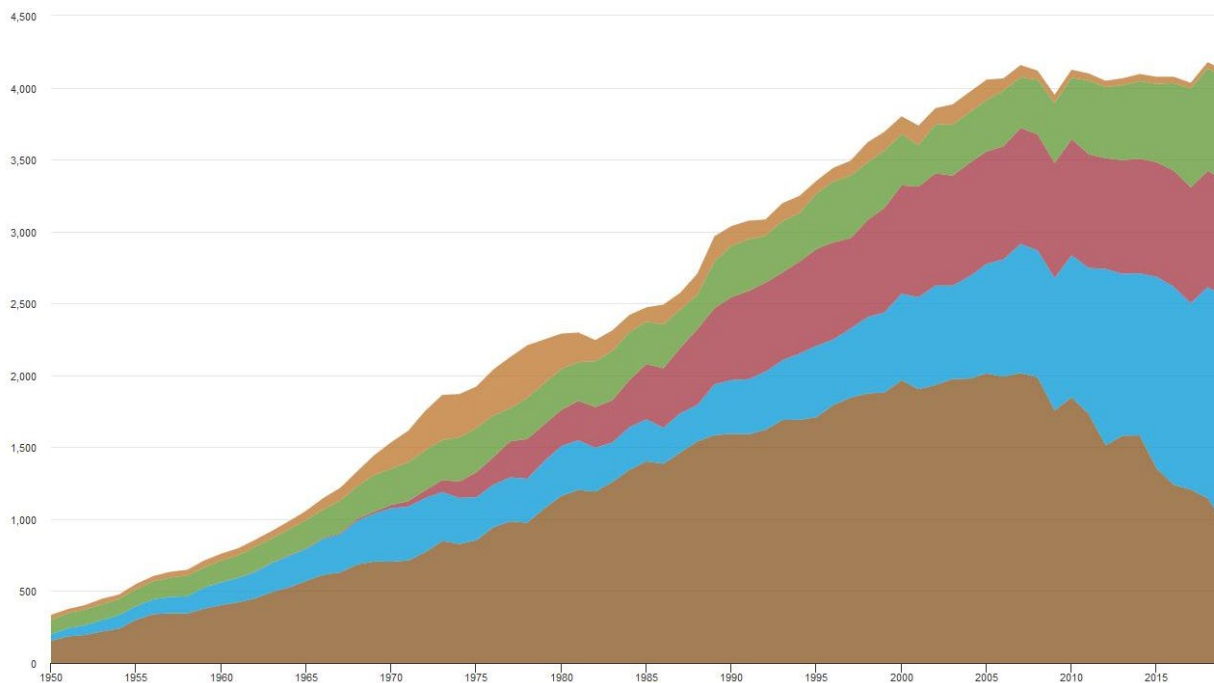


Figure 2: US electricity generation by energy source from 1950 to 2020, Colors: Dark brown – Coal, Blue – Natural Gas, Red – Nuclear, Green – Renewables, Tan – Petroleum [1]

One of the reasons gas turbines have been a popular energy solution is due to their low NO_x , or nitrogen-oxide gas, emissions and high efficiency. For example, the GE-EDF combined-cycle plant in Bouchain, France has been recognized by the Guinness World Records as the most efficient combined-cycle power plant in the world with a thermal efficiency of $\sim 62.2\%$ [3]. Efficiency of this magnitude was previously unheard of when using coal, with the most efficient coal-fired plant reaching $\sim 45\%$ at J-Power's Isogo Thermal Power Station [4] Natural gas turbines not only achieve top-of-the-line efficiency, but they do so while also emitting very low NO_x and CO_2 into the environment [5] Higher efficiency equates to less CO_2 emissions due to modern gas turbines' ability to burn at higher firing temperatures than previous turbine iterations.

Most combined cycle power plants accomplish pollutant removal with a catalyst. The process works similarly to a catalytic converter in a car. Exhaust gas containing NO_x enters a heat recovery steam generator (HRSG) and is mixed with ammonia and other compounds to chemically remove the harmful products before they can enter the environment [6]. NO_x is a key component of smog, highly corrosive, and contribute to the greenhouse effect [7].

However, low- NO_x combustors have significant thermoacoustic stability issues, particularly the coupling between the flame and the acoustic field. This coupling will be expanded further in the Literature Review chapter of this thesis. One of the drivers of instability in gas turbine combustion systems is the flow field, so changes to the fuel injection hardware inside the combustor can have significant impacts on the flow field and thus combustion instability [8]. The goal of this work is to understand the impact that the addition of a centerbody, which is a common feature in power-generation gas turbine fuel injectors, has on the fluid mechanic instabilities that can drive overall thermoacoustic instability [9].

This thesis is organized as follows. Chapter 2 explains the current literature on the subject of fluid dynamics, swirling flows, and gas turbines and ends with the gaps that exist in the literature that pertain to centerbodies in gas turbine combustors. Chapter 3 establishes the setting and what tools will be used to run the experiment. Chapter 4 discusses the acoustic characterization of the test rig without a centerbody and how that pertains to the overall experiment. Chapter 5 explains the results of the research and chapter 6 concludes the thesis with a synthesis of how the results build upon existing theory and what future work can be done.

Chapter 2

Literature Review

Gas turbine combustors combine compressed air and fuel and ignite the mixture to create high-energy exhaust that turn bladed rotors and generate power. Shown in Figure 3 is an example of a Siemens gas turbine with the combustor system expanded.

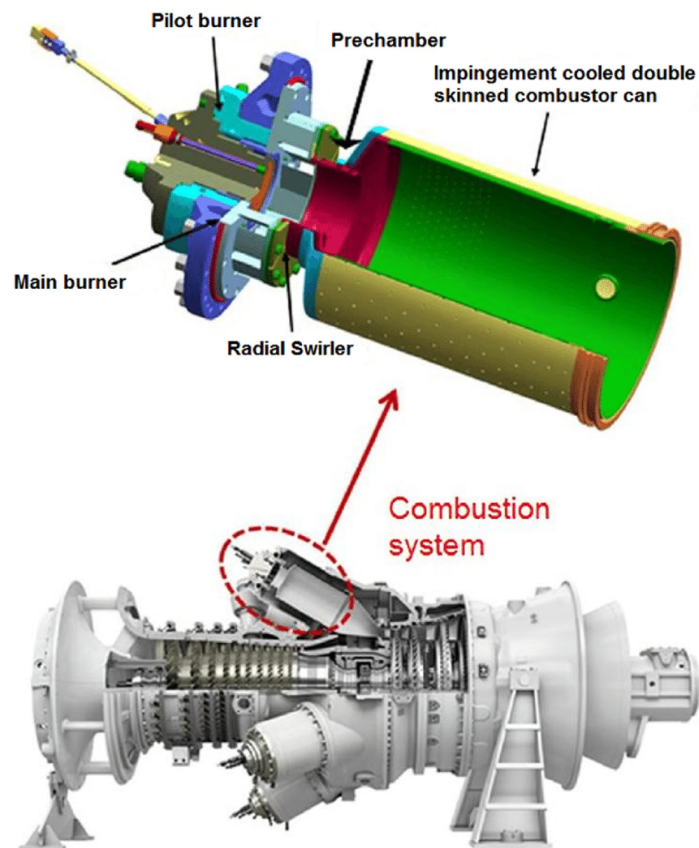


Figure 3: Swirling flow combustor in a Siemens gas turbine [10]

In a conventional gas turbine, atmospheric pressure air enters the front of the turbine in the compressor section, upstream of the combustion system. This air is compressed to high pressures to ensure plenty of oxygen is in a compact space. Fuel, usually natural gas or jet fuel is injected into the combustion system along with the compressed air and is ignited to create high-pressure, high-temperature exhaust. Inside the combustor, the fuel/air mixture flows through a swirler where it starts to rotate, increasing mixing; the role of swirl will be further explained later in the literature review. The swirling flow of air and fuel moves to the main combustion chamber or combustion can, illustrated by the green section of Figure 3, where it fully forms into high-pressure and high-temperature exhaust. This exhaust then moves to the turbine section where the pressure drops and the gas flow turns large blades, shown downstream of the combustion system. In power generation, the turbine shaft is connected to a generator, and as it spins will generate electricity for the power grid.

The focus of this thesis is in the combustor section of the gas turbine and how changing the flow in the combustor impacts combustor performance. Almost all gas turbine combustors use swirlers to mix the fuel and air, and many, particularly in power-generation gas turbines, use centerbodies, or bluff-bodies located in the center of the swirling flow to help stabilize the flame. These assemblies change the flow patterns and structures in many ways and are good for flame stabilization and mixing.

Swirling Flow

Used predominantly in gas turbine combustors, swirling flows are employed to stabilize combustion, mix air and fuel, and as a result of the patterns it creates in the flow, emit less pollutants, like NO_x , into the atmosphere. There are two typical swirler geometries – radial-flow and axial-flow swirlers. As shown in Figure 4, gas enters the rectangular channels and mixes with the centrally flowing air. This swirling will create a tornado-like pattern in the combustion chamber.



Figure 4: Axial-Flow Swirler [11]



Figure 5: Radial-Flow Swirler [11]

Swirling flows have different structures of interest, including shear layers and recirculation zones. How these structures form and interact are essential to understand regarding swirling flow. Figure 6 outlines these structures in non-reacting swirling flow.

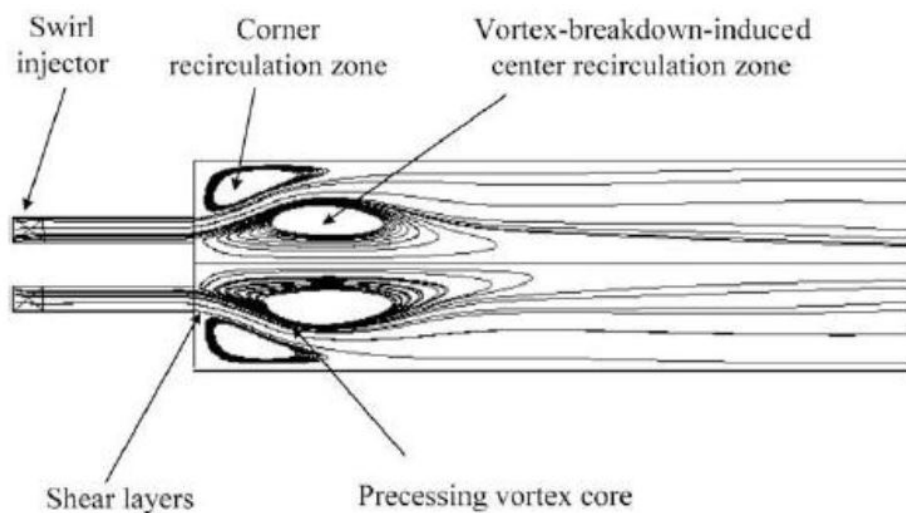


Figure 6: Non-reacting swirling flow with key structures outlined [12]

Recirculation zones are pockets of reverse flow where flames can stabilize inside combustion chambers and be continuously fed by the air/fuel mix without being extinguished [13]. Note, that corner recirculation zones assist with fuel mixing but are impractical for flame stabilization because of their proximity to the walls that promote heat loss from the flame, thus flames usually stabilize in the central recirculation zones. Shear layers, as shown by Figure 6, are areas of high velocity gradients between recirculation zones and the swirling jet that aid in fuel/air mixing and flame stabilization.

The central recirculation zone of a swirling flow is a result of a process known as vortex breakdown [14]. Vortex breakdown occurs when the ratio of swirling velocity (azimuthal) to axial velocity reaches a critical value. When this ratio is reached, the flow becomes unstable because of

the low-pressure core of the jet and the jet collapses into itself, resulting in a large recirculation zone along the centerline of the flow. This vortex breakdown is what causes flame stabilization and enhanced air and fuel mixing [15].

Two forms of vortex breakdown are likely to occur in a flow stream: Figure 7 is the bubble-type breakdown, or spiral breakdown. The bubble form is characterized by a stagnation point in the center of the swirling jet, creating the bubble, followed by a corkscrew pattern downstream. Figure 8 shows the spiral form of vortex breakdown, where the stagnation point occurs, again, along the centerline but the flow instability is not strong enough to cause full flow reversal [16]. Though the spiral form breakdown is uncommon in gas turbine combustors, the bubble-type breakdown is found in almost all modern combustor designs.

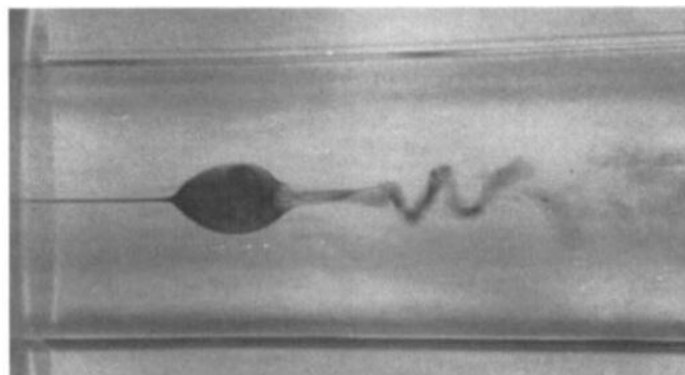


Figure 7: Bubble-form vortex breakdown [16]

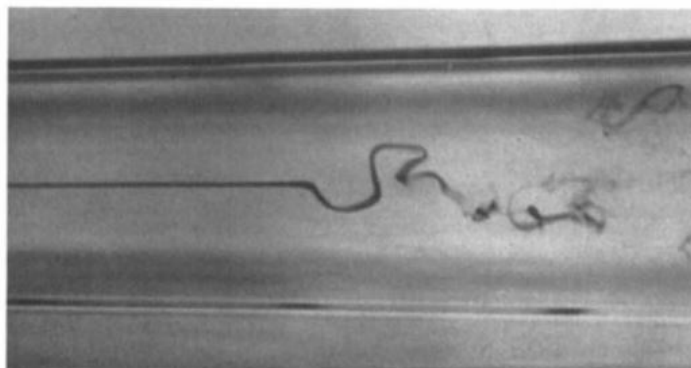


Figure 8: Spiral-form vortex breakdown [16]

Vortex breakdown bubbles do not necessarily stay stationary in the flow. Oscillation of the vortex breakdown bubble is called a precessing vortex core (PVC) [15]. The PVC present causes the swirling flow to be three-dimensional as a result of the highly non-axisymmetric motion of the precessing vortex breakdown bubble [13].

Precessing Vortex Cores in Swirling Flows

The precessing vortex core (PVC) is a vortex breakdown phenomenon responsible for areas of intense mixing in swirling flow combustors [17]. The PVC appears when a swirl-generated central recirculation zone forms and becomes unstable, resulting in the core to precess around the centerline of the flow [17]. The precession results in a helical structure in the shear layers surrounding the vortex core as a result of the large-scale disturbances that the core precession causes. Figure 9 shows a rendering of the three-dimensional shape of the pressure field caused by the PVC. The blue helix structure is the PVC disturbance field, the gold lines represent air-fuel mixture flow, and the toroidal vortex structure represents the central recirculation zone [15].

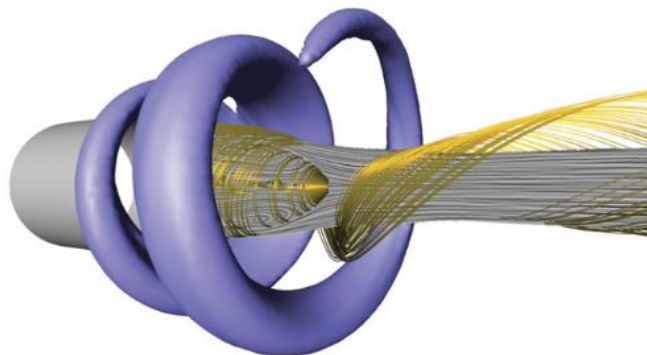


Figure 9: 3D Illustration of PVC [15]

In a combustor, the PVC achieves increased flame stabilization by recycling hot combustion gases back into the base of the flame as new fuel and air are injected into the system and it also improves flame anchoring in the central recirculation zone [18]. The PVC increases the turbulence and shear at the edge of the recirculation zone mixing the air and fuel. This increased turbulence and shear, combined with gas recycling, leads to efficient burning of low-quality fuels like low calorific value natural gas and high-sulfur coal [19]. However, the PVC can also cause large-scale disturbances in the flame, which can lead to issues of combustion instability [20], described next. Other research, however, shows that the PVC may actually be able to suppress these harmful combustion instabilities [21]. Given these conflicting results, the role of the PVC in combustor stability and operation is still a rich area for research.

Combustion Instability

Swirling flows can be unstable, which have potentially damaging implications for the operations of a gas turbine. In particular, combustion instability, which is a feedback loop between combustor acoustics and heat release rate oscillations, can cause reduced combustor operability, increased emissions, and component damage. Figure 10 shows the structure of this feedback cycle. Here, flame heat release rate oscillations feed energy into the combustor acoustic field. These acoustic oscillations then excite oscillations in a variety of coupling mechanisms, which further drive heat release rate fluctuations.

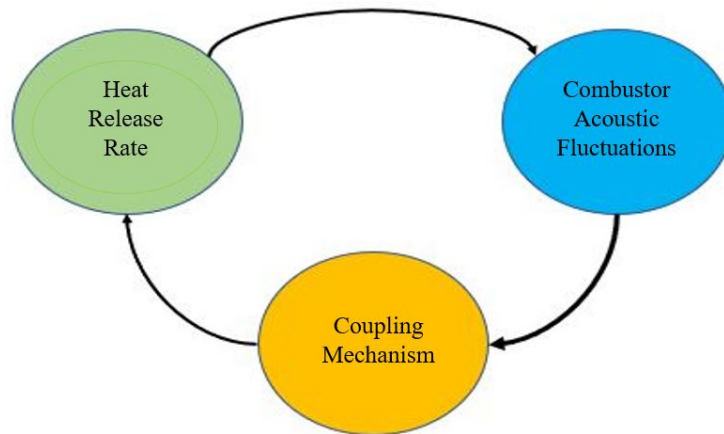


Figure 10: Combustion instability feedback loop

Combustion instability can occur and be exacerbated by different coupling mechanisms. One such mechanism is the relation of heat release fluctuations and velocity fluctuations, driven by oscillations in the acoustic field. A rapidly changing flame surface, caused by perturbations in the swirling air/fuel flow, generates intense sound and can feed energy into a resonant mode if the two disturbances are in phase. This feedback of flow perturbations changing the flame surface and generating potentially resonant frequencies is an example of an instability driving mechanism, shown in Figure 11.

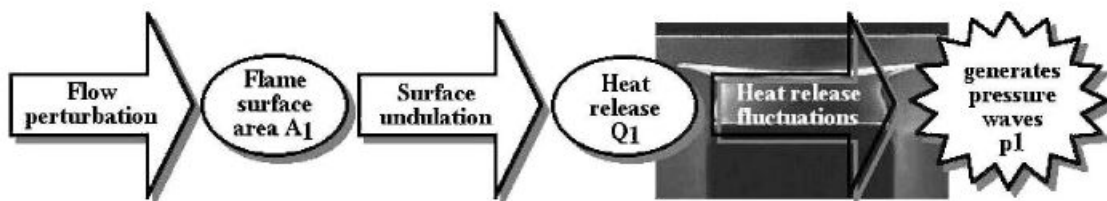


Figure 11: Driving mechanism resulting in pressure waves [22]

Instabilities resulting from resonance between driving processes lead to flow oscillations. These oscillations lead to many problems in turbines – including structural vibrations, increased

heat flux, flashback (when the flame propagates into the swirler), and flame blowoff (when the flame loses stabilization and propagates into the turbine) [22]. Figure 12 illustrates some of the coupling mechanisms that can come about from pressure-induced acoustic waves resulting from the driving mechanism. As shown in part (a) of Figure 12, acoustic wave motion induces a fluctuation in velocity, which causes a flow modulation and a fluctuation in flame surface area. This fluctuation in flame surface area causes an unsteady heat release and completes the feedback loop.

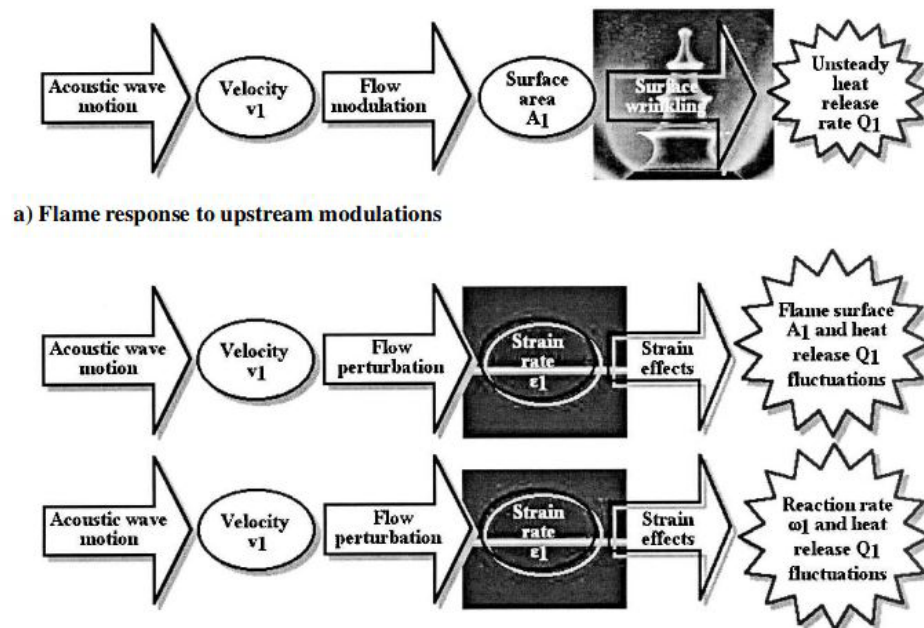


Figure 12: Example of a coupling mechanism [22]

Unsteady heat release can cycle back and excite more flow perturbations and thus create a combustion instability cycle. To avoid these instabilities, we need to understand the mechanisms behind them and how they change when the structure of the flow changes due to variations in the combustor geometry, including changes in swirl number and centerbody geometry [23].

Centerbodies

The focus of this work is to understand the impact of a centerbody on the precessing vortex core and the response of the flow to acoustic perturbations, as would be present during combustion instability. Centerbodies are used in many different combustor designs to enhance flame stabilization in two ways. First, they promote additional recirculation in the wake of the centerbody, leading to stronger reverse flow and supply of hot, chemically active products to the flame base. Second, they create low velocity, separating shear layers from the centerbody that promote flame stabilization at the end of the centerbody. Centerbodies can take many different shapes, but commonly they are cylinders placed downstream of the swirler. The centerbody allows a centrally located recirculation zone to form that is not swirl-dependent. Instead of relying on the swirling flow to generate unsteady recirculation zones, the centerbody forces a recirculation zone to occur where designers want one. This allows a flame sit centrally in the combustor and the swirling flow around the centerbody enhances the central zone [24]. Figure 13 shows different recirculation zones that can form from a centerbody in different swirl number conditions. The patterns displayed in cases (a) through (i) occur with increasing swirl number.

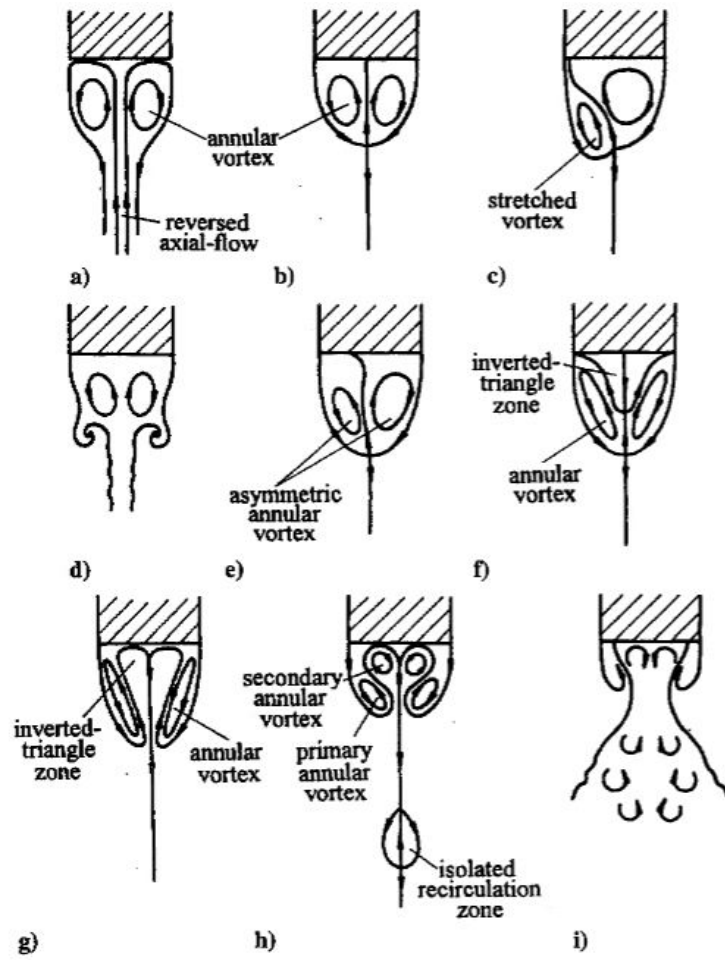


Figure 13: Recirculation zone patterns due to an axially placed centerbody, as case number increases, swirl number increases and changes the flow response [24]

Gaps in the Literature

To date, the literature has shown that the structure of swirl flows is highly dependent on the geometry of the combustor. Swirl-dependent central recirculation zones form downstream of the swirler at the onset of vortex breakdown. Oscillation of the vortex-breakdown bubble is called a precessing vortex core, which improves flame stabilization and mixing, but can cause large-scale flame disturbances, leading to combustion instability. Centerbodies can force a central recirculation zone to form according to designer specifications and can improve flame stabilization due to the recirculation of chemically active combustion products to the flame base.

One of the major remaining questions is about how the centerbody shape affects the dynamics of the PVC. Recent simulations by Mukherjee *et al.* [25] have shown that changing the width of the centerbody can suppress the PVC – increasing the centerbody width decreases the energy in the precessing vortex core. However, no published experimental work on this topic exists. In this work, experiments will be performed in varying swirl and Reynolds number conditions with centerbodies of different diameters to test Mukherjee’s hypotheses in the lab. Proper Orthogonal Decomposition (POD) will be used to discern frequencies showing the presence of a PVC. The pressure data generated will either support or reject the present theory regarding centerbody influence on PVC dynamics. Further, the Reacting Flow Dynamics Laboratory has a long-standing collaboration with the group at the Indian Institute of Science – Bangalore from Mukherjee *et al.*, and the results of this experimental work will be used to further verify these preliminary findings from simulation.

Chapter 3

Experimental Methods

Experimental Facility

The goal of this facility is to simulate and study swirling air flow that would enter a gas turbine combustor. Pressure data of the air exiting the top of the rig is recorded and analyzed to determine the presence of the precessing vortex core and how it acoustically changes depending on different flow and swirl conditions. Figure 14 shows the rig designed to accurately study swirling flows of air and mimic the air-flow function of a gas turbine combustor.

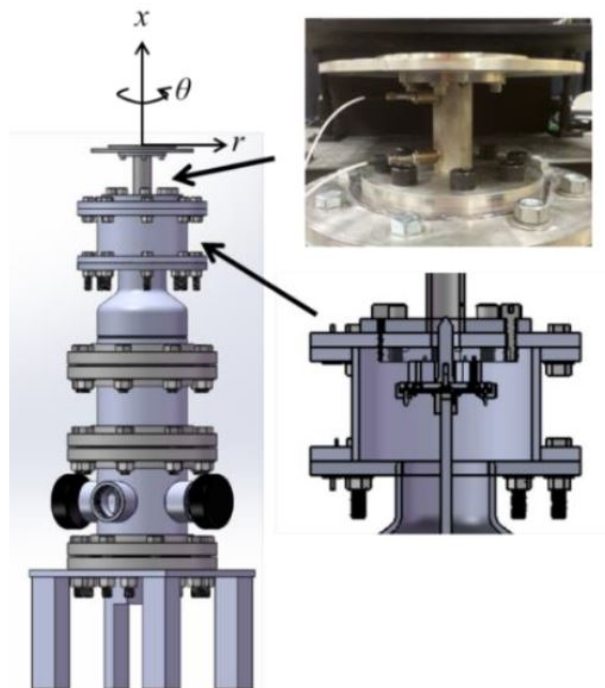


Figure 14: Swirling flow testing rig with x , r , and θ as the axial, radial, and azimuthal axes, respectively [26]

The rig consists of three sections: a settling chamber where air coming in from the inlet hose passes through two perforated plates before it enters the swirler. Shown in the bottom right of Figure 14, air enters the swirler and now has a swirling velocity component in addition to the axial component. The swirler is a radial-entry swirler that has eight NACA 0015 airfoil blades [26]–[28]. The trailing edge of the blades are pinned to the swirler case plates and the front of the blades are attached to a pin that is rotated by the dual-plate configuration that rotates to change the blade angle depending on the desired level of swirl. The airfoils are driven in-tandem by a stepper motor connected to the shaft at the bottom of the swirler. The blade angle can be adjusted between -65° and $+65^\circ$ with each step correlating to a 2.5° change in angle. Figure 15 shows a CAD rendering of the swirler internals.

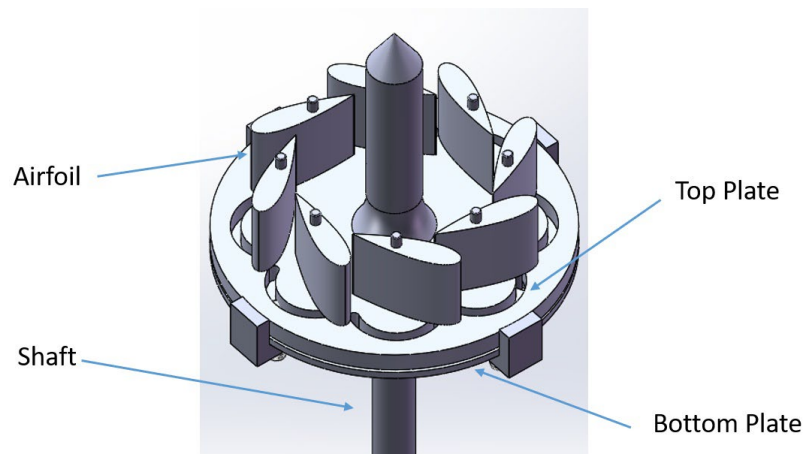


Figure 15: Swirler [28]

With the aid of a centerbody, the swirling jet enters the exit nozzle shown in the top right of the figure and is shot out of the top of the rig. As the flow passes through the nozzle, it encounters two PCB 113B28 differential pressure transducers [26]. The volumetric flow rate is recorded using a Thermal Instruments 600-9 thermal mass flow meter.

New Centerbody Design

For this work, new centerbodies were designed to understand the impact of centerbody size and location relative to the dump plane on precessing vortex core dynamics. Four new centerbodies were designed using the criteria shown in Table 1. The baseline centerbody has a diameter of $D = 1$ inch and its trailing edge is flush with the dump plane, as shown in Figure 16. The length of this baseline centerbody is 4.5 inches.

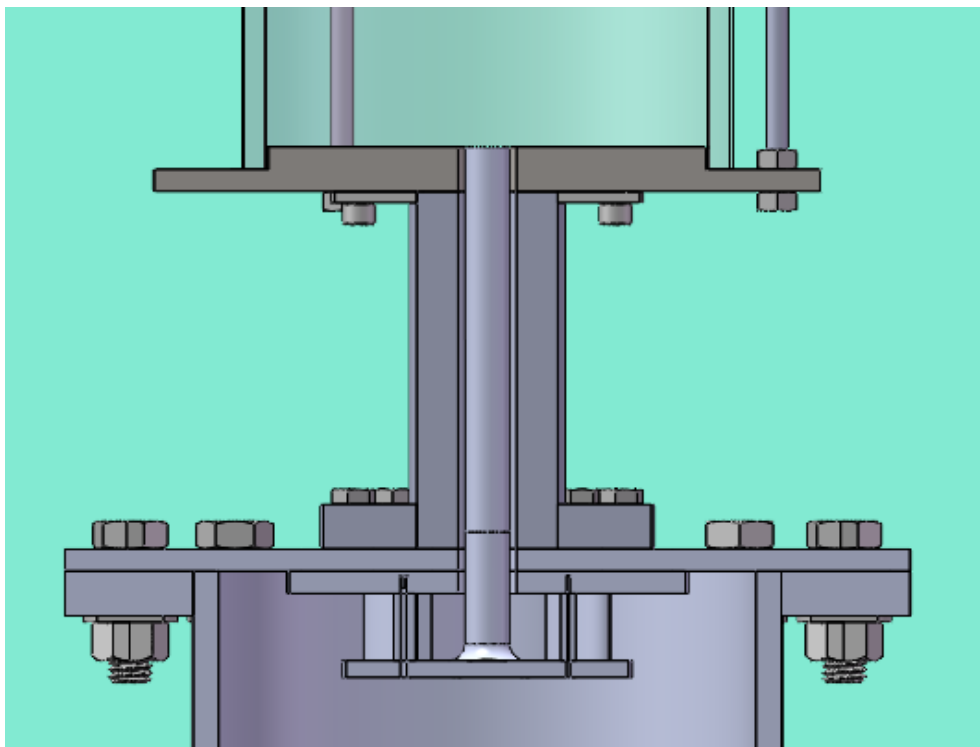


Figure 16: Cutaway of the swirl rig with the baseline centerbody

Tapered centerbodies with a $0.5D$ trailing-edge diameter were designed because halving the diameter reduces the width and length of the central wake recirculation zone (CWRZ) [29]. This reduction in length and width that forces the vortex breakdown bubble (VBB) and the CWRZ to separate could potentially impact the effect of a centerbody on the PVC instability; though the separation of the VBB and CWRZ is dependent on swirl number [29]. The new

centerbodies will be recessed 0.4 inches for the odd-numbered centerbodies, and the even-numbered ones will protrude 0.4 inches from the dump plane. Moving the centerbody with respect to the dump plane changes the location of the CWRZ relative to the VBB, which can change their interaction and hence the PVC dynamics. The distances relative to the dump plane were chosen based on previous work by Frederick [28], who mapped the flow field of the time-average flow field as a function of swirl number at the baseline flow condition of 30 SCFM. The location of $0.4D$ downstream of the dump plane is where the base of the VBB is at inception of the PVC at a swirl number of $S = 0.79$, making it an interesting length scale for investigating the role of the centerbody in this study.

The centerbodies attach to the swirler by a threaded connection. The centerbody screw-end diameter is 0.5 inches, and the tapered centerbody exit-end diameter is $0.5D$ or 0.25 inches. Figures 17 and 18 show CAD renderings of a tapered and non-tapered centerbody, respectively.

Table 1: Centerbody Design Criteria

Length:	4.1"	4.9"
Tapered:	CB 3	CB 4
Non-Tapered:	CB 1	CB 2

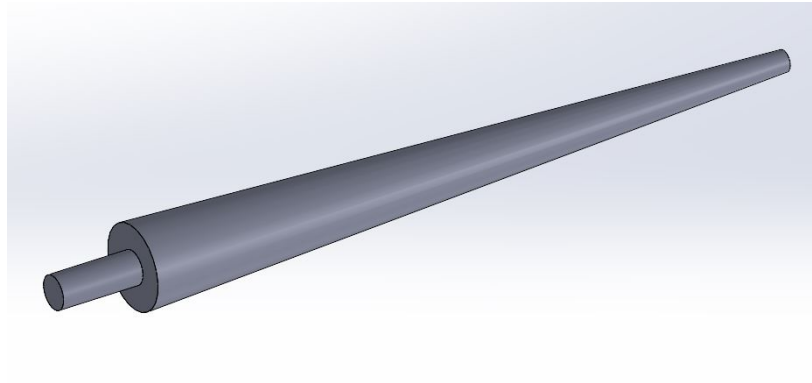


Figure 17: Tapered Centerbody (Recessed 0.4")

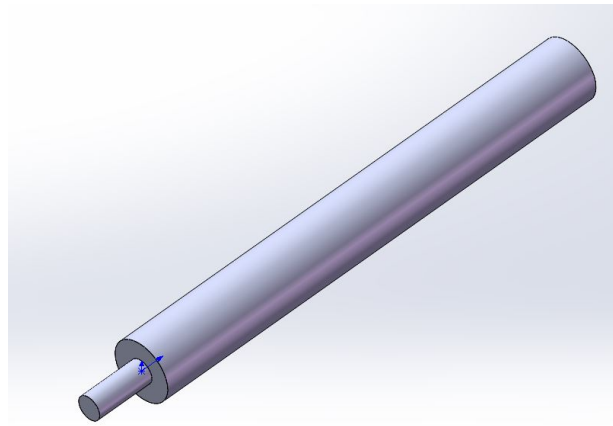


Figure 18: Non-tapered Centerbody (Recessed 0.4")

Diagnostics and Data Analysis

In this work, the acoustic pressure in the nozzle is measured using two piezoelectric pressure transducers mounted on the rig exit nozzle. Data is obtained using a National Instruments CompacRIO data acquisition system at a sampling rate of 20 kHz with 3 seconds of data collection resulting in 60,000 data points which recorded and averaged into 6 ensembles. Using MATLAB, the ensembles are converted to a frequency spectrum using the MATLAB FFT command, and the resulting graph shows RMS pressure vs. frequency.

Chapter 4

Acoustic Characterization of the Non-Centerbody Case

Acoustic excitation disturbs and manipulates swirling flows and fluctuations in these acoustics are a key component of the instability feedback loop shown in Figure 10. In industrial gas turbines or other environments pertaining to combustion, the acoustic resonances in the system can have a significant impact on the dynamical behaviors of the flow and the flame. Work completed by Frederick [28] identified the acoustic resonances of the current experiment by performing a frequency sweep with the two forcing sirens located at the bottom of the rig and measuring the pressure fluctuations at the two nozzle transducer locations for two swirl numbers. Figure 19 shows the acoustic characterization of the experimental rig, indicating that the experimental rig without a centerbody has acoustic resonances at 720, 1060, and 1320 Hz. Note that the acoustic resonance frequencies do not change with blade angle. The first two resonance modes at 720 and 1060 Hz are displayed by the two pressure transducers at the same amplitude, meaning these are long wavelength modes present in the entire rig. The higher frequency modes present beyond 1320 Hz differ between the two pressure transducers meaning the mode is likely resonating within the nozzle itself rather than throughout the whole rig.

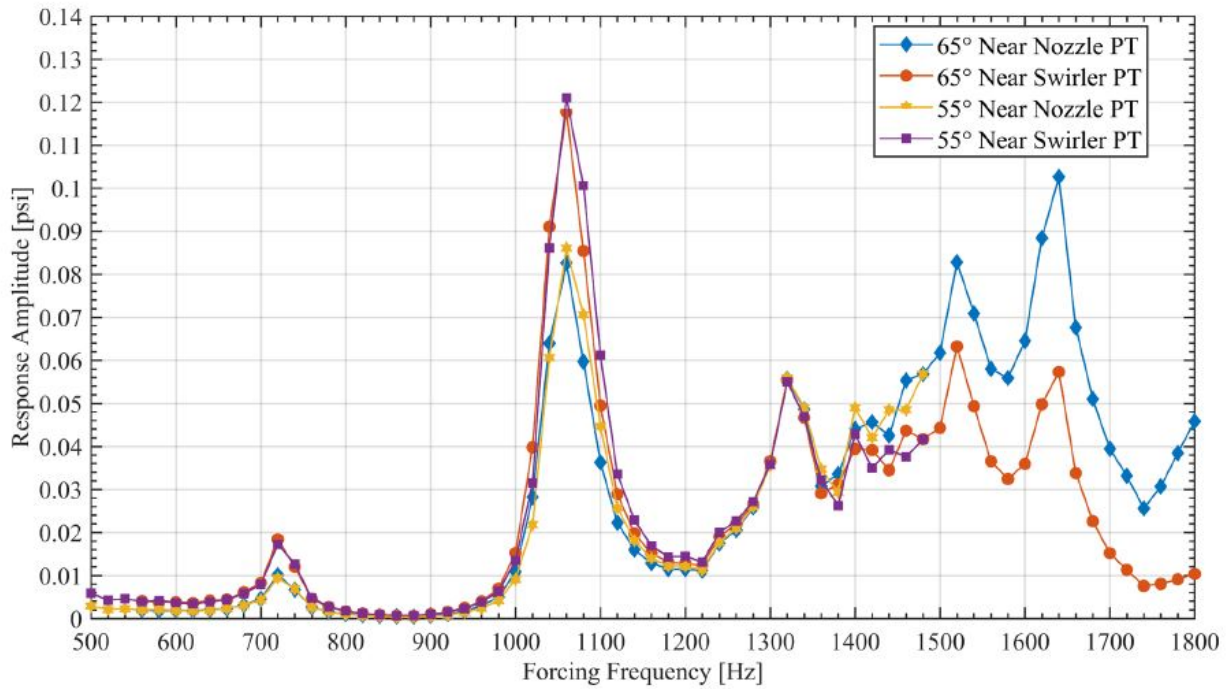


Figure 19: Acoustic characterization of rig done by Frederick [28]

A study was done to determine if the PVC frequencies determined by Frederick remained constant over time. The study was replicated at a blade angle of 65° at different bulk flow velocities. Figure 20 shows Frederick's acoustic data at a 65° blade angle and different flow

velocities. Figure 21 shows the pressure power spectral density response of the flow at different velocities taken for this experiment.

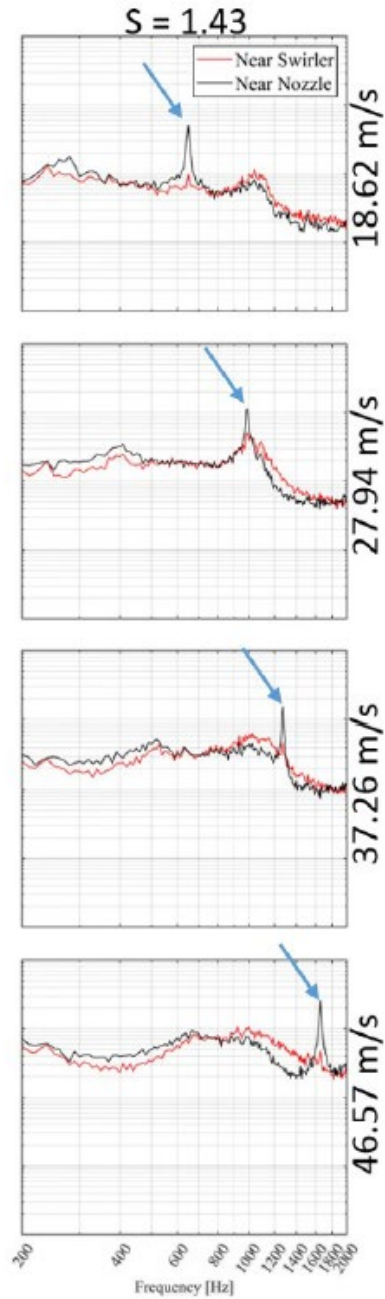


Figure 20: Acoustic response of the PVC at 65-degree BA and various flow velocities [28]

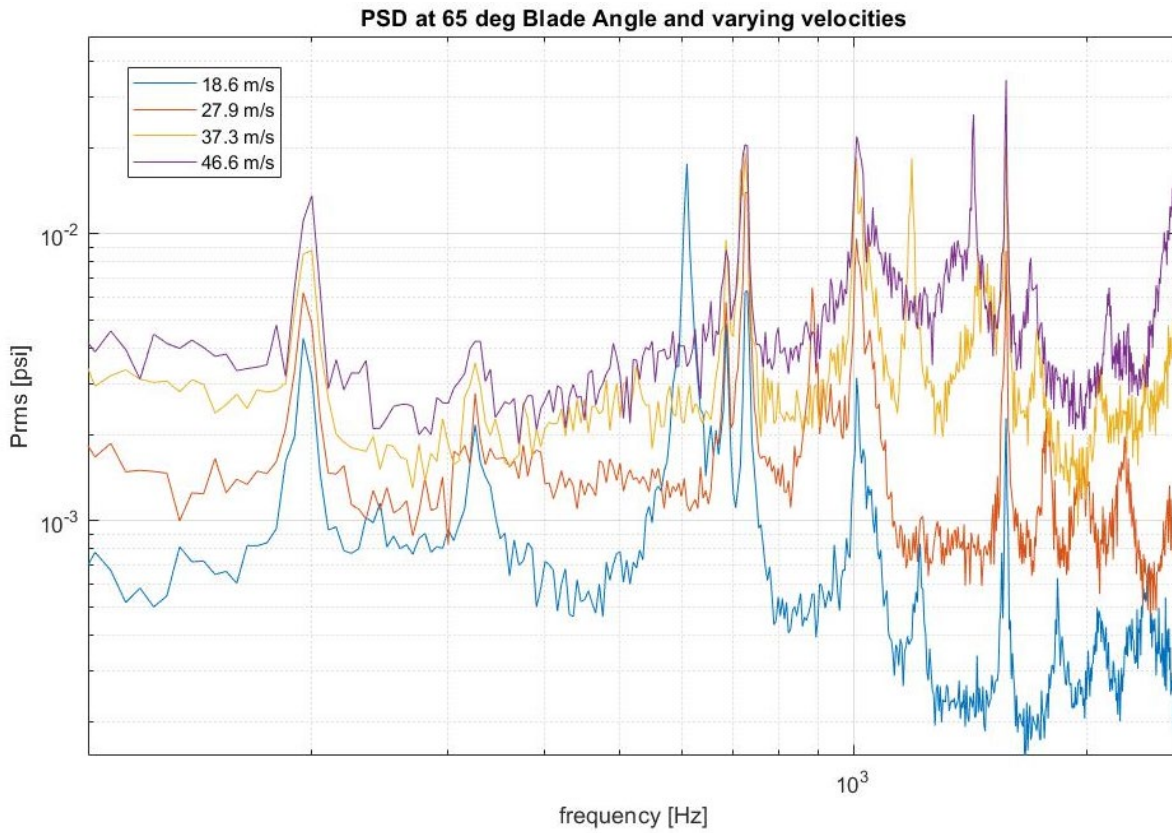


Figure 21: PSD Frequency Response

Figure 21 shows that the flow is noisier than the previous acoustic characterization in Figure 20. In this study, peaks that remain at a constant frequency as the flow velocity is changed are acoustic resonances because their frequency is governed by the size of the experiment, not the flow velocity (in the low Mach number limit). Table 2 shows the expected PVC frequencies at different swirl numbers.

Table 2: Frederick Test Matrix [28]

Swirl number	Flow state	PVC frequency
0.00	No VB	—
0.18	No VB	—
0.38	No VB	—
0.56	Intermittent VB	—
0.79	Weak PVC	770–815 Hz
1.05	PVC	840 Hz
1.43	Strong PVC	1060 Hz

According to Frederick's data, a strong PVC should exist at the 65° blade angle case at 1060 Hz – a resonance frequency of the rig. The peaks in Figure 20 correspond to this expected value in the 37.3 m/s and 46.6 m/s cases, as the PVC is shown to occur at 1040 – 1080 Hz.

Peaks that move with flow velocity are likely the result of fluid mechanic instability as the frequency of the instability changes with flow velocity. Instead, fluid mechanic instabilities typically display at constant Strouhal number. The Strouhal number is a non-dimensional frequency derived using a characteristic length, L , and flow velocity, U . For a jet, the characteristic length would be the jet diameter and the characteristic velocity would be the bulk flow velocity.

$$St = \frac{fL}{U} \quad (1)$$

The precessing vortex core frequencies were largely repeatable from Frederick's data [28]. The PVC was not strong at the 20 SCFM case. As flow increased, the PVC frequency also increased. According to Figure 21, the PVC exists at 900 Hz for the 27.9 m/s case, at 1040 Hz for the 37.3 m/s case, and at 1060 Hz in the 46.6 m/s case, respectively. Both the 27.9 and 37.3 m/s cases agree with the expected PVC frequency at $S = 1.43$ shown in Table 2.

The length used for calculating the Strouhal number was the diameter of the nozzle, 1 inch, and is identical in each flow case. As the flow rate increases, the PVC frequency increases, but the Strouhal number plot shows that the non-dimensional frequency remains about the same. This similarity was also demonstrated in Frederick.

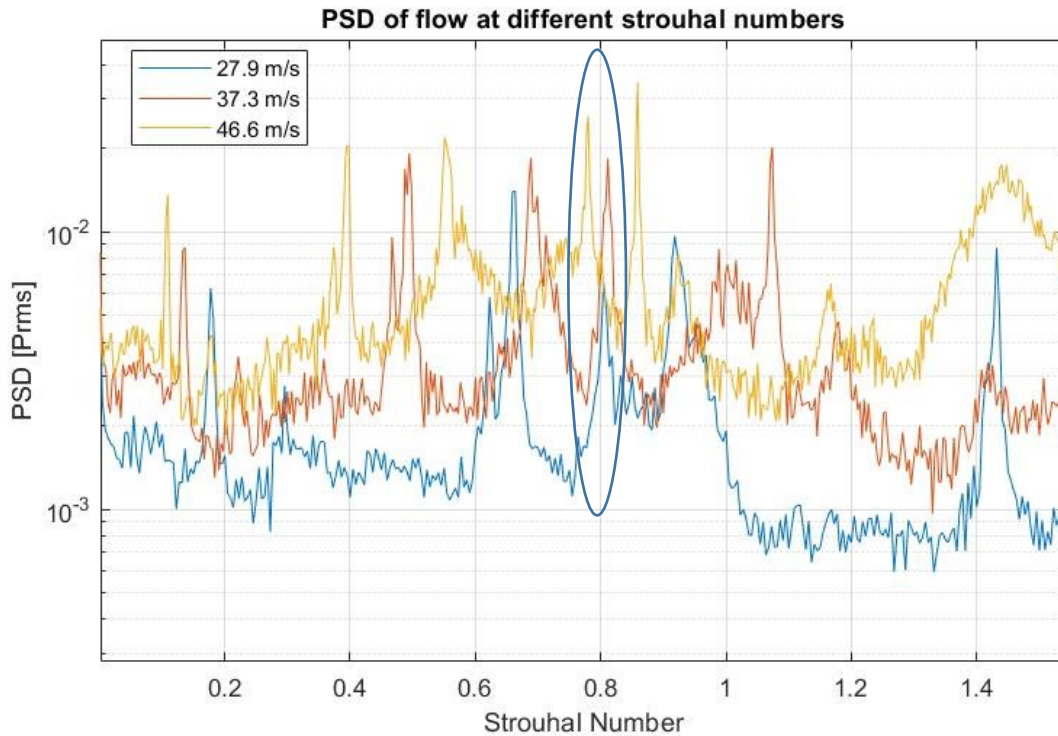


Figure 22: Non-centerbody acoustic response vs. Strouhal number at $S = 1.43$

Note that the PVC stays around the same Strouhal number of 0.8 at the different flow cases, as noted by the oval in Figure 22. This Strouhal number corresponds with data taken by Frederick, as the Strouhal number in that study was 0.88 [28]. The PVC also increases in magnitude as flow velocity increases. The 18.6 m/s case was omitted since a PVC is not expected to exist at this flow velocity and blade angle. The next chapter will discuss performing a similar acoustic characterization using the designed centerbodies specified in Table 1. Centerbodies are able to suppress the PVC according to Mukherjee *et al.* [29], so the expectation is that there will be no PVC signatures in the pressure data.

Chapter 5

Acoustic Characterization with Centerbodies

This chapter focuses on characterizing the acoustic response of the rig at different swirl conditions using the centerbodies discussed in Table 1. From Mukherjee's theory [29], the expected result is that the PVC will disappear or diminish in magnitude when the flow is exposed to centerbodies of different lengths and diameters. This is because the centerbody disrupts the wavemaker region at the base of the vortex breakdown bubble, which drives PVC oscillations.

The non-tapered centerbody pressure data will be presented and analyzed in the first section followed by the tapered centerbody data in the second section. For this work, two volumetric flow case will be examined: 22.5 SCFM, with the non-tapered centerbodies, and 29.5 SCFM with the tapered centerbodies. These flow rates were chosen because the annulus diameter with the centerbody reduces the cross-sectional area compared to the no-centerbody case. Factoring in the annulus area, 22.5 and 29.5 SCFM result in a bulk flow velocity of 27.94 m/s – identical to the 30 SCFM no-centerbody case. A blade angle sweep will be performed at a constant bulk flow velocity of 27.94 m/s. The sweep will focus on high-swirl cases where a PVC is most likely to occur. Table 3 shows the test matrix for each centerbody. The swirl numbers were selected to draw comparisons between data taken by Frederick for acoustic characterization without a centerbody at an analogous flow rate.

Table 3: Test matrix for acoustic characterization with centerbodies

Centerbody:	1	2	3	4	
Flow Rate (m/s):	27.94				Swirl Number
	55	55	55	55	0.95
Blade Angle (deg):	60	60	60	60	1.15

To determine the differences between the recessed and protruded centerbodies and how they influence the flow, the cases were plotted together at 55-degree and 60-degree blade angles.

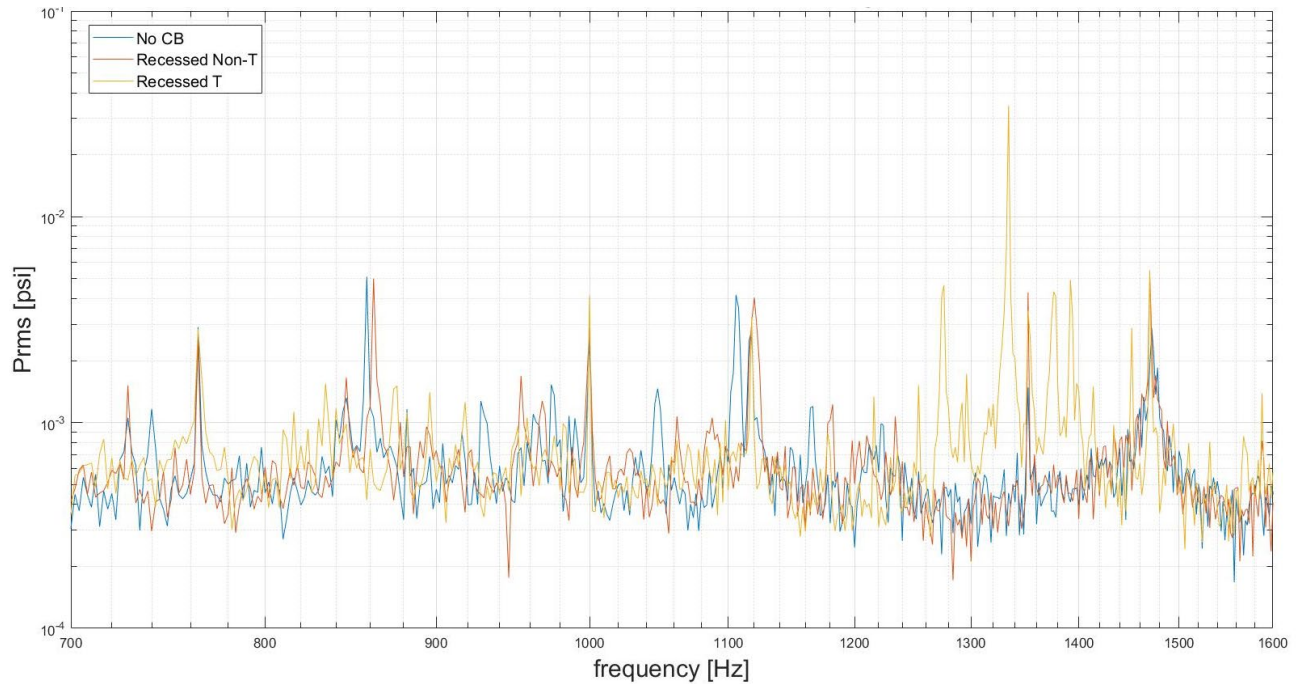
**Figure 23:** Recessed centerbody comparison at $S = 0.95$

Figure 23 has peaks at 760, 860, 1000, 1100, 1360, and 1470 Hz. The peak at 860 Hz matches with the expected PVC frequency at $S = 0.95$. The peaks at 760, 1100, and 1360 Hz correspond with resonances shown in Figure 19. The PVC frequency of 860 Hz is present in both the no centerbody case and the non-tapered, recessed centerbody case, but not the tapered centerbody. The peak in the tapered case at 1340 Hz is amplified, as the rig has non-negligible resonance at this frequency. The peak present in all cases at 1470 Hz does not match with the

previous acoustic characterization. This peak is likely an acoustic resonance given its frequency and the multiple peaks seen in the acoustic characterization in Figure 19.

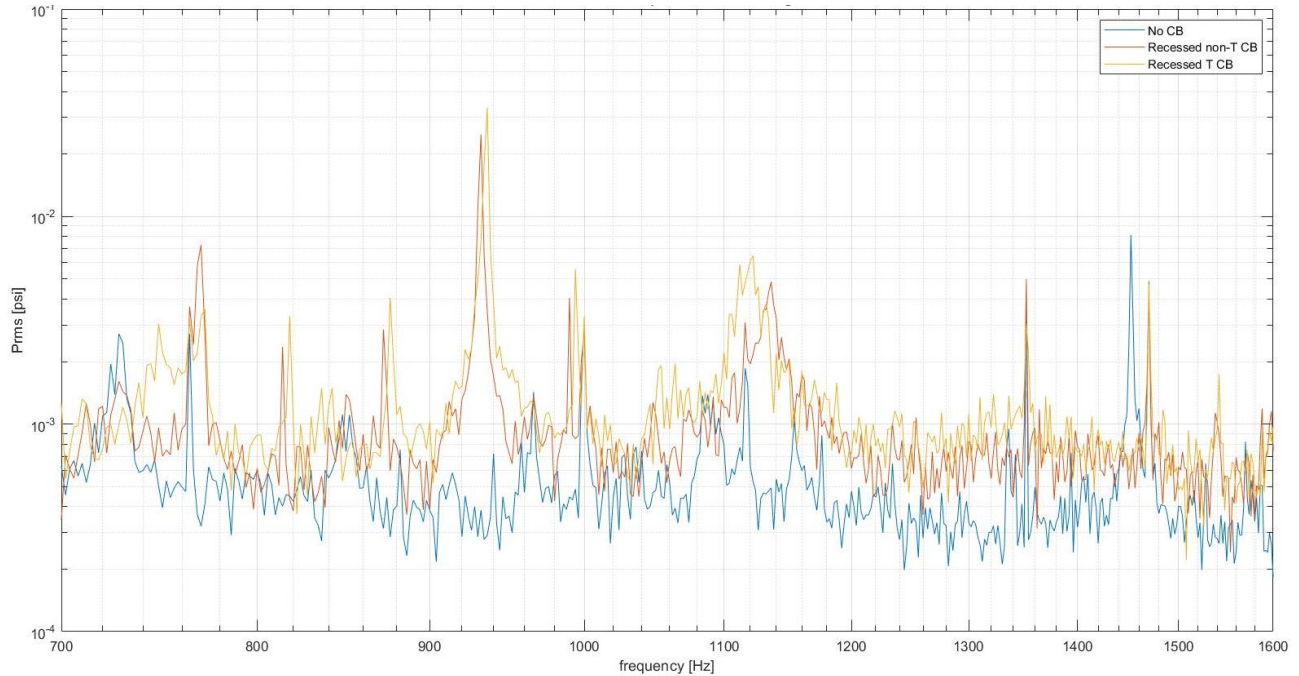


Figure 24: Recessed centerbody comparison at $S = 1.15$

Figure 24 shows the pressure spectrum for the recessed centerbodies at a swirl number of $S = 1.15$, and has peaks at 760, 820, 940, 1000, 1120, 1360, and 1470 Hz. The expected PVC frequency at $S = 1.15$ is ~ 940 Hz which can be seen at 960 Hz for the no centerbody case and, similarly to Figure 23, is amplified instead of attenuated. However, even in the tapered case, the PVC is amplified. The peaks at 760, 1120, and 1360 Hz correspond to the resonance frequencies of the rig. Frequencies between 1000 and 1140 Hz are amplified considerably, as this is the main resonance frequency of the rig. Similar to Figure 23, the 1470 Hz spike does not converge in the acoustic characterization for all cases, so this mode may be dynamic and correspond to different swirl numbers.

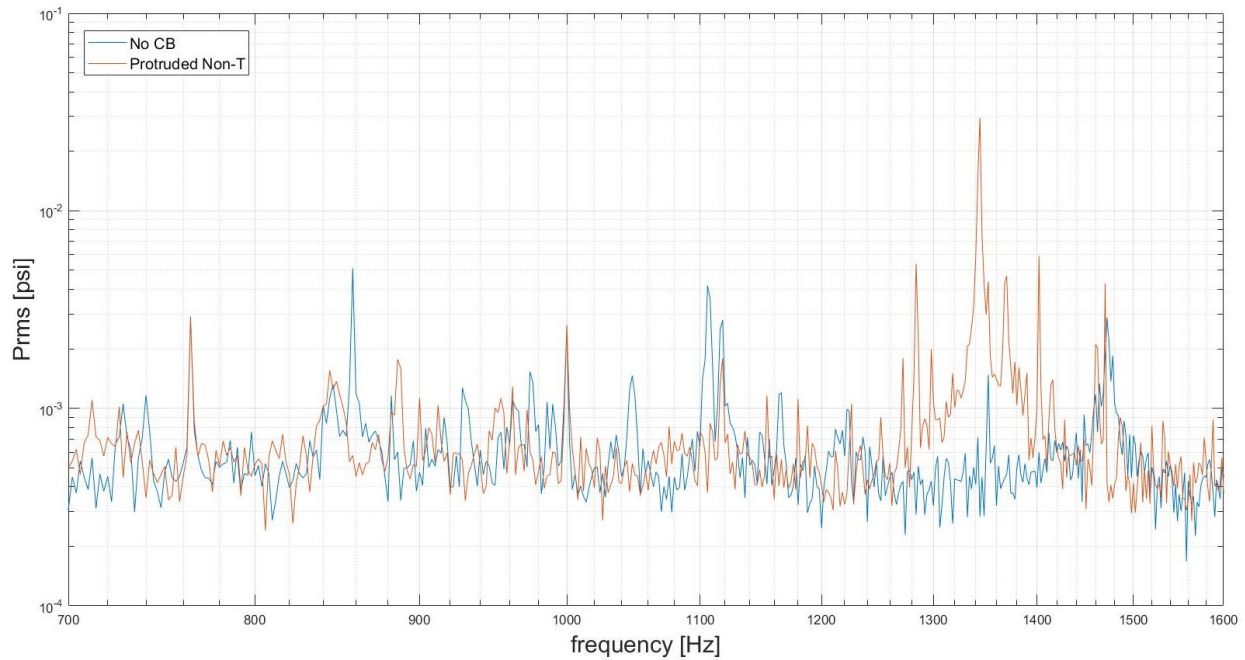


Figure 25: Protruded centerbody compared to base case at $S = 0.95$

Figure 25 shows the pressure spectrum for the protruded, non-tapered centerbody at $S = 0.95$ as compared to the no centerbody case. The expected PVC frequency at this swirl number is ~ 840 Hz, which is noted by the blue peak at this frequency. The other peaks at 720, 1000, 1120, and 1360 Hz, like in Figure 23 and Figure 24, correspond to resonance frequencies of the rig and are present in all pressure readings. For the protruded centerbody case, the PVC at 840 Hz was successfully dampened. This case agrees with Mukherjee [29] who states that protruding a centerbody at the base of the vortex breakdown bubble would disrupt the wavemaker region and suppress the PVC. However, the 1360 Hz signal was amplified considerably compared to the no centerbody case. Protruded centerbody data was unable to be taken at $S = 1.15$ for the non-tapered case and at any swirl number for the tapered case due to clipping of the voltage signal from the data acquisition system used.

Chapter 6

Conclusions and Future Work

The goal of this work was to better understand how centerbodies of different designs affect the PVC. Centerbody dimensions were determined to protrude $0.4D$ from the dump plane in centerbodies 2 and 4 from Table 1, and recess $0.4D$ into the dump plane based on results from Frederick [28]. To discern the effects both protruded and recessed centerbodies had on the PVC, pressure spectra were developed using data at a flow rate of 30 SCFM and swirl numbers of $S = 0.95$ and $S = 1.15$. The pressure spectra showed whether the centerbodies amplified or suppressed the PVC present at each swirl number.

The recessed non-tapered centerbody failed to suppress the PVC at $S = 0.95$, but the tapered centerbody did. At $S = 1.15$, neither centerbody suppressed the PVC present at ~ 940 Hz. The protruded centerbody successfully suppressed the PVC at $S = 0.95$. These results show that the wavemaker region must be directly disturbed by a protruding centerbody, not indirectly disturbed by a recessed centerbody, in order for the PVC to be suppressed. This experimental work is an important step in confirming the postulated theory in Mukherjee *et al.* [29] and better understanding of the effect of injector design choices on the dynamics of swirling flows in gas turbine combustors.

More experimental work needs to be done to effectively characterize centerbody influence on the precessing vortex core, especially at high-swirl cases ($S = 1.43$). Results of this work could have implications in combustor design to include centerbodies protruding from the dump plane, as the protruded case eliminated the PVC. Protruding the centerbody could influence the central recirculation zone which could be determined using particle image velocimetry (PIV).

Next steps for the swirl experiment would be to use PIV to effectively diagnose the conditions of the acoustic field at high-swirl cases where a PVC would be present using the centerbodies studied in this work, specifically centerbodies 2 and 4. PIV is a high-speed laser diagnostic technique used to render an image of the flow field and measure different components of velocity. A high-powered laser sheet is used to illuminate particles that have been mixed into the swirling jet ahead of the settling chamber of the rig.

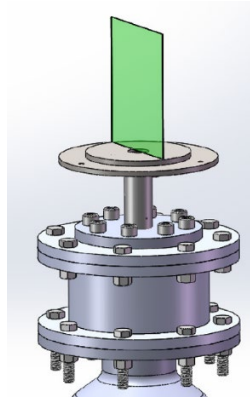


Figure 26: Particle image velocimetry in the r - x plane [28]

Using PIV to analyze high-swirl cases with different centerbodies would assist in better understanding how centerbodies of different designs impact the flow field and the PVC. Through this method, the high-swirl flow could be determined and different centerbody designs could be tested to see how they affect the central recirculation zone. This recirculation zone is a region of low-velocity flow and is important to understand because it is what allows flames to be stable and not be extinguished inside of gas turbine combustion chambers [9], [17]. Beyond characterizing the flow, further work could be done using flames to experimentally derive the influence of centerbodies on combustion instability through their PVC dampening capabilities.

As gas turbines continue to provide clean and efficient power for a growing population, continuous improvements need to be made when designing these machines and their supporting systems. As such, centerbodies need to be further understood and iterated upon to further improve combustor performance and by extension, that of the overall gas turbine.

BIBLIOGRAPHY

- [1] R. Berry, “Electricity Monthly Update for November 2020,” *Electric Power Monthly*, no. November 2020, 2021.
- [2] N. Sonnichsen, “Natural Gas vs. Coal Price per million BTU,” 2020. <https://www.statista.com/statistics/189180/natural-gas-vis-a-vis-coal-prices/> (accessed Feb. 19, 2021).
- [3] A. Larson, “World’s Most-Efficient Combined Cycle Plant: EDF Bouchain,” *POWER*, Sep. 2017.
- [4] R. Peltier, “Top Plant: Isogo Thermal Power Station Unit 2, Yokohama, Japan,” *POWER*, no. October, 2010, [Online]. Available: https://www.powermag.com/top-plantisogo-thermal-power-station-unit-2-yokohama-japan/?itm_source=parsely-api.
- [5] W. C. Pfefferle, “Method for Obtaining Ultra-Low NO_x Emissions from Gas Turbines Operating at High Turbine Inlet Temperatures,” United States Patent 7765810 B2, 2010.
- [6] IST, “Heat Recovery Steam Generators,” 2019. <https://otsg.com/industries/powergen> (accessed Feb. 19, 2021).
- [7] J. Seinfeld and S. Pandis, *Atmospheric Chemistry and Physics: From Air Pollution to Climate Change*, 2nd ed. Hoboken, New Jersey: John Wiley & Sons, 2006.
- [8] T. Lieuwen, B. Zinn, V. Yang, “Combustion Instabilities: Basic Concepts,” in *Combustion Instabilities In Gas Turbine Engines*, Reston ,VA: American Institute of Aeronautics and Astronautics, 2006, pp. 3–26.

- [9] P. Heberling, M. Kelsey, and W. Dodds, "Cyclonic Prechamber with a Centerbody for a Gas Turbine Engine Combustor," United States Patent 5540056, 1996.
- [10] F. E. Agbonzokilo, I. Owen, J. Stewart, S. K. Sadasivuni, M. Riley, and V. Sanderson, "Experimental and Numerical Investigation of Fuel–Air Mixing in a Radial Swirler Slot of a Dry Low Emission Gas Turbine Combustor," *Journal of Engineering for Gas Turbines and Power*, vol. 138, no. 6, Jun. 2016, doi: 10.1115/1.4031735.
- [11] C. Hirsch, D. Fanaca, P. Reddy, W. Polifke, and T. Sattelmayer, "Influence of the Swirler Design on the Flame Transfer Function of Premixed Flames," in *Volume 2: Turbo Expo 2005*, Jan. 2005, doi: 10.1115/GT2005-68195.
- [12] S. Wang, S.-Y. Hsieh, and V. Yang, "Unsteady flow evolution in swirl injector with radial entry. I. Stationary conditions," *Physics of Fluids*, vol. 17, no. 4, p. 045106, Apr. 2005, doi: 10.1063/1.1874892.
- [13] N. Syred and J. M. Beér, "Combustion in swirling flows: A review," *Combustion and Flame*, vol. 23, no. 2, pp. 143–201, 1974, doi: 10.1016/0010-2180(74)90057-1.
- [14] T. Sarpkaya, "On stationary and travelling vortex breakdowns," *Journal of Fluid Mechanics*, vol. 45, no. 3, pp. 545–559, Feb. 1971, doi: 10.1017/S0022112071000181.
- [15] K. Oberleithner *et al.*, "Three-dimensional coherent structures in a swirling jet undergoing vortex breakdown: stability analysis and empirical mode construction," *Journal of Fluid Mechanics*, vol. 679, pp. 383–414, Jul. 2011, doi: 10.1017/jfm.2011.141.
- [16] S. Leibovich, "The structure of vortex breakdown," *Annual Review of Fluid Mechanics*, vol. 10 pp. 383-414, 1978, doi: 10.1090/gsm/146/03.

- [17] N. Syred, W. Fick, T. O'Doherty, and A. J. Griffiths, "The Effect of the Precessing Vortex Core on Combustion in a Swirl Burner," *Combustion Science and Technology*, vol. 125, no. 1–6, pp. 139–157, May 1997, doi: 10.1080/00102209708935657.
- [18] S. Candel, D. Durox, T. Schuller, J.-F. Bourgoign, and J. P. Moeck, "Dynamics of Swirling Flames," *Annual Review of Fluid Mechanics*, vol. 46, no. 1, pp. 147–173, Jan. 2014, doi: 10.1146/annurev-fluid-010313-141300.
- [19] D. Froud, "Phase averaging of the precessing vortex core in a swirl burner under piloted and premixed combustion conditions," *Combustion and Flame*, vol. 100, no. 3, pp. 407–410, Feb. 1995, doi: 10.1016/0010-2180(94)00167-Q.
- [20] A. M. Steinberg, I. Boxx, M. Stöhr, C. D. Carter, and W. Meier, "Flow-flame interactions causing acoustically coupled heat release fluctuations in a thermo-acoustically unstable gas turbine model combustor," *Combustion and Flame*, vol. 157, 2010, pp. 2250–2266, doi: 10.1016/j.combustflame.2010.07.011.
- [21] M. Frederick, K. Manoharan, J. Dudash, B. Brubaker, S. Hemchandra, and J. O'Connor, "Impact of Precessing Vortex Core Dynamics on Shear Layer Response in a Swirling Jet," *Journal of Engineering for Gas Turbines and Power*, vol. 140, no. 6, Jun. 2018, doi: 10.1115/1.4038324.
- [22] S. Ducruix, T. Schuller, D. Durox, and S. Candel, "Combustion Dynamics and Instabilities: Elementary Coupling and Driving Mechanisms," *Journal of Propulsion and Power*, vol. 19, no. 5, pp. 722–734, Sep. 2003, doi: 10.2514/2.6182.
- [23] A. Lacarelle *et al.*, "Spatiotemporal Characterization of a Conical Swirler Flow Field Under Strong Forcing," *Journal of Engineering for Gas Turbines and Power*, vol. 131, no. 3, May 2009, doi: 10.1115/1.2982139.

- [24] H. J. Sheen, W. J. Chen, and S. Y. Jeng, "Recirculation zones of unconfined and confined annular swirling jets," *AIAA Journal*, vol. 34, no. 3, pp. 572–579, Mar. 1996, doi: 10.2514/3.13106.
- [25] A. Mukherjee, N. Muthichur, C. More, S. Gupta', and S. Hemchandra, "The Role of the Centerbody Wake on the Precessing Vortex Core Dynamics of a Swirl Nozzle," *ASME Turbo Expo*, GT2020, no. 15777, 2020.
- [26] S. Clees, "The Onset of Vortex Breakdown in Swirling, Turbulent Jets," Undergraduate Honors Thesis 2018.
- [27] B. Mathews, "Combustor Flow Field Characterization with Acoustic Forcing and Swirl Fluctuations," Undergraduate Honors Thesis 2015.
- [28] M. Frederick, "Natural Dynamics of a Precessing Vortex Core in Swirling Flows," Undergraduate Honors Thesis 2018.
- [29] Mukherjee, A., Muthichur, N., More, C., Gupta, S., & Hemchandra, S. (2021). The Role of the Centerbody Wake on the Precessing Vortex Core Dynamics of a Swirl Nozzle. *Journal of Engineering for Gas Turbines and Power*, 143(5), 051019.

Academic Vita

Jackson T. Horigan

EDUCATION

The Pennsylvania State University, University Park PA **Graduation: May 2021**
Schreyer Honors College
Bachelor of Science in Mechanical Engineering

Humanitarian Engineering and Social Entrepreneurship Program

ShambaTek Irrigation Venture – Kisumu, Kenya January 2021 – May 2021

Dean's List (All Semesters) August 2017 – May 2021

President's Freshman Award April 2018

Research Assistant – Reactive Flow Dynamics Laboratory August 2019 – May 2021
Dr. Jacqueline O'Connor, Ph.D.

Honors Thesis:

Understanding Impacts of Centerbodies on the Precessing Vortex Core in Swirling Flow

EMPLOYMENT EXPERIENCE

ExxonMobil (Oil & Gas):

Machinery Engineering Co-Op - Beaumont Chemical Plant, TX August – December 2020

Dominion Energy (Electric Utility):

Mechanical Engineering Intern - Mount Storm Generating Station, WV May – July 2019

Mechanical Engineering Intern - Bear Garden Generating Station, VA May – July 2018

COMPUTER PROFICIENCIES

MATLAB, C++, Python, Inventor, SolidWorks, LabVIEW, PI Processbook, EtaPro

CLUBS & ACTIVITIES

Statesmen A-Capella – Baritone

Penn State Chanoyu Club – Urasenke Japanese Tea Ceremony

Penn State Chess Club

Penn State Swing Dance Club